Early View publication on www.interscience.wiley.com
(issue and page numbers not yet assigned;
citable using Digital Object Identifier – **DOI**)

Phys. Status Solidi B, 1–4 (2009) / **DOI** 10.1002/pssb.200880543

physica status solidi b
www.pss-b.com
basic solid state physics

# Hybrid reflections in InGaP/GaAs(001) by synchrotron radiation multiple diffraction

**Alan S. de Menezes[1], Adenilson O. dos Santos[1], Juliana M. A. Almeida[1], José R. R. Bortoleto[2], Mônica A. Cotta[1], Sérgio L. Morelhão[3], and Lisandro P. Cardoso[*, 1]**

[1] IFGW, Universidade Estadual de Campinas-UNICAMP, CP 6165, 13083-970 Campinas, SP, Brazil
[2] Engenharia de Controle e Automação, Unesp, 18087-180 Sorocaba, SP, Brazil
[3] Instituto de Física, Universidade de São Paulo, CP 66318, 05315-970 São Paulo, SP, Brazil

Received 7 July 2008, revised 7 November 2008, accepted 7 November 2008
Published online 17 December 2008

**PACS** 41.60.Ap, 61.05.cp, 68.35.bg, 68.35.Dv, 81.15.Hi

[*] Corresponding author: e-mail cardoso@ifi.unicamp.br, Phone: +55 19 3521 5500, Fax: +55 19 3521 5376

Hybrid reflections (HRs) involving substrate and layer planes (SL type) [Morelhão et al., Appl. Phys. Lett. **73** (15), 2194 (1998)] observed in Chemical Beam Epitaxy (CBE) grown InGaP/GaAs(001) structures were used as a three-dimensional probe to analyze structural properties of epitaxial layers. A set of (002) rocking curves ($\omega$-scan) measured for each 15° in the azimuthal plane was arranged in a pole diagram in $\phi$ for two samples with different layer thicknesses (#A – 58 nm and #B – 370 nm) and this allowed us to infer the azimuthal epilayer homogeneity in both samples. Also, it was shown the occurrence of $(1\bar{1}3)$ HR detected even in the thinner layer sample. Mappings of the HR diffraction condition ($\omega$:$\phi$) allowed to observe the crystal truncation rod through the elongation of HR shape along the substrate secondary reflection streak which can indicate in-plane match of layer/substrate lattice parameters.



**1 Introduction** The most important application of X-ray scattering in the investigation of semiconductor materials is for feedback on crystal growth, ex-situ. The method does not harm the sample, is reasonably fast, allows the information to be available in minutes and has a very high sensitivity to composition determination. In many ways the approach is rather direct, the composition relates directly to the expansion or contraction of the lattice (Vegard's law) and because of the very high strain sensitivity, the composition can be extracted to high precision. The shape of the scattering peaks also relates to the layer thickness, effectively diffraction broadening, and thickness interference fringing can occur. Therefore, the X-ray scattering pattern contains information on the composition and thickness of layers.

A very useful technique which presents resolution and sensitivity high enough for the analysis of materials is X-ray Multiple Diffraction, in particular for semiconductors materials. This technique is very sensitive to small variations on lattice parameters and it has also been successfully applied in the study of piezoelectricity of several crystals [1–6]. For semiconductors, it has been applied to the study of ion implanted semiconductors [7, 8] and epitaxial layered heterostructures, in which the lattice of the layer and substrate can be studied separately, just by selecting one adequate layer or substrate peak. In the analysis of heterostructures, a special diffracted reflection from the substrate (layer) lattice can appear at certain experimental condition and can be chosen to provide simultaneous information on both lattices (layer and substrate). These are called hybrid reflections [9]. They carry information of the two lattices because they are different sequences of reflections inside the layer/substrate structure. In the model of consecutive diffractions, the secondary planes within the substrate (layer) lattice diffract the primary beam towards the coupling planes which are in the layer (substrate) lattice. Since both lattices contribute to the multiple diffracted beam one can simultaneously obtain information of these lattices. Two special hybrid reflections have already been obtained for the $In_{0.49}Ga_{0.51}P$/GaAs(001) system, using a (002) primary reflection and they have provided very high sensitivity in the analysis of the substrate miscut and interface distance in epitaxial growth and therefore, for that case, they were called coherent hybrid reflection (CHR) [10].

In the present work, the layer thickness effect in the $In_{1-x}Ga_xP/GaAs(001)$ semiconductor structure is discussed in detail through observed hybrid reflections (HR), which can be presented in a pole diagram to allow for a visualization of the HR peak distribution. These reflections can give simultaneous information on epilayer/substrate lattices. Furthermore, the mapping of the HR diffraction condition can give information on the HR shape and intensity as a function of the layer thickness.

**2 X-ray multiple diffraction** The multiple diffraction phenomenon arises when an incident beam simultaneously satisfies the Bragg law for more than one set of lattice planes within the crystal. For this, the plane called primary ($h_o$, $k_o$, $l_o$) is adjusted to diffract the incident beam. With the rotation ($\phi$ angle) of the sample around the primary reciprocal lattice vector, several other planes called secondary ($h_s$, $k_s$, $l_s$) and coupling ($h_o - h_s$, $k_o - k_s$, $l_o - l_s$), will also enter in diffraction condition simultaneously with the primary. These coupling planes establish the interaction between the primary and the secondary reflections. In the pattern $I_{primary}$ *versus* $\phi$, called Renninger Scan (RS) [11], positive and negative (dip) secondary peaks can appear distributed according to the symmetry of the primary vector, representing the energy transfer from the secondary to the primary reflection (peak) and vice-versa (dip) and, also considering the symmetry plane established by the $\phi$ rotation. The secondary peak position in the RS is given by $\phi = \phi_o \mp \beta'$ and the $\mp$ signal defines the entrance and the exit of the secondary reciprocal lattice point of the Ewald Sphere by rotation. $\phi_o$ is the angle between $\boldsymbol{H}_\perp$ (component of $\boldsymbol{H}$ on a plane perpendicular to $\boldsymbol{H}_o$) and $\boldsymbol{H}_{Ref}$, the reference vector. Three-beam X-ray diffractions in single crystals are excited when the incident beam (wavevector $\boldsymbol{k}$) fulfills two Bragg conditions:

$$\boldsymbol{k} \cdot \boldsymbol{H}_o = -\boldsymbol{H}_o \cdot \frac{\boldsymbol{H}_o}{2} \tag{1}$$

and

$$\boldsymbol{k} \cdot \boldsymbol{H}_s = -\boldsymbol{H}_s \cdot \frac{\boldsymbol{H}_s}{2} \ . \tag{2}$$

Since $\boldsymbol{H}_o = \boldsymbol{H}_s + \boldsymbol{H}_c$, we also have

$$\boldsymbol{k} \cdot \boldsymbol{H}_c = -\boldsymbol{H}_c \cdot \frac{\boldsymbol{H}_c}{2} - \boldsymbol{H}_c \cdot \boldsymbol{H}_s \ , \tag{3}$$

where $\boldsymbol{H}_o$, $\boldsymbol{H}_s$ and $\boldsymbol{H}_c$ are the primary, secondary and coupling reciprocal lattice vectors, respectively. The hybrid reflections, whose secondary and coupling planes are not in the same lattice, are illustrated in Fig. 1, where one can see the two types of possible hybrid reflections, labeled as LS and SL [12]. These hybrids are specified by their sequence of reflections, it means, when the secondary plane is in the substrate lattice and the coupling plane is in the layer lattice, one has the SL hybrid case (Fig. 1a). Otherwise, when the coupling plane is in the substrate lattice and the secondary plane is in the layer lattice, one has the LS hybrid case (Fig. 1b). It is worthwhile to point out that it is possible to predict the exact incidence angle ($\omega$) and azimuthal angle ($\phi$) of the hybrid reflections as demonstrated by Morelhão and Domagala [13].

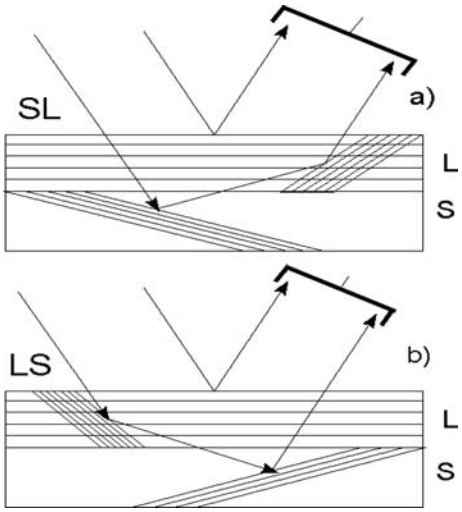


**Figure 1** Scheme of the hybrid reflections in an epitaxial structure: a) SL and b) LS paths.

**3 Experimental** $In_{1-x}Ga_xP$ epilayers were grown by chemical-beam epitaxy (CBE) on semi-insulating GaAs(001) substrates. Trimethylindium and triethylgallium, with $H_2$ as a carrier gas, were used as group-III sources. Thermally cracked $AsH_3$ and $PH_3$ were used as group-V sources. The substrate native oxide was removed by heating the sample at 600 °C under $AsH_3$ overpressure. Two samples, labeled #A and #B, with different epilayer thicknesses of 50 nm and 400 nm, respectively, have been investigated here. A 300 nm GaAs buffer, growth rate of 0.72 μm/h, precedes the $In_{1-x}Ga_xP$ epilayers, which were grown at a rate of 0.95 μm/h in both samples. The growth temperature was 550 °C for buffers and epilayers.

X-ray multiple diffraction measurements were carried out at station XRD1 of the Laboratório Nacional de Luz Síncrotron (LNLS), Campinas, SP, Brazil. The wavelength used in our experiments was 1.5495(1)Å. A beam size of the order of 1.0 mm × 1.0 mm was defined on the sample surface. The Huber three-axis diffractometer used in the experiments is mounted at station XRD1 of the LNLS, and provides high resolution measurements with step sizes of 0.0002° in both $\omega$- and $\phi$-axis.

**4 Results and discussion** Rocking curves (RCs) using the symmetric 002 reflections for #A and #B samples were performed at $\phi = 0°$ ([110] direction) as can be seen in Fig. 2, while thickness, composition and perpendicular lattice parameters extracted by data fitting [14–17] are given in Table 1.

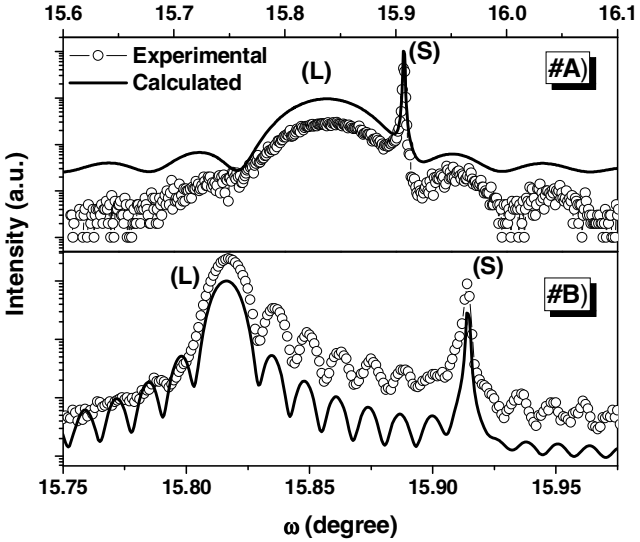


**Figure 2** Synchrotron radiation rocking curves of #A and #B samples with their corresponding calculation. The substrate (S) and layer (L) peaks are indicated.

Pole diagrams composed of 25 of these RCs, set apart by 15° in phi, were obtained to inspect the epilayer quality as well as to evidence the occurrence of hybrid reflections that can be excited near the chosen phi angles. The HR we have chosen to measure is due to the four-beam case, it means, it involves the reflections [incident (000), primary (002), secondary ($1\bar{1}\,\bar{1}$) and secondary ($1\bar{1}3$)]. However, in order to occur the SL hybrid has to follow the path $(1\bar{1}3)_S + (\bar{1}1\bar{1})_L$ according to the Fig. 1a.

Figure 3 shows the pole diagrams of the #A and #B samples. One can observe in each pole diagram the presence of substrate and layer contributions and also the hybrid indicated by arrows following the 4-fold symmetry of the primary reflection vector together with the contributions of the symmetry plane provided by the entrance and exit of the reciprocal lattice point from the Ewald sphere. Furthermore, in this figure are shown the RCs of the #A sample obtained at $\phi = 0°$ and $\phi = 30°$ that is close to the calculated position of the ($1\bar{1}3$) HR indicated in the figure ($\omega = 15.945°$ and $\phi = 30.197°$).

Figures 4 and 5 show $\omega:\phi$ mappings of the exact diffraction condition of the ($1\bar{1}\,\bar{1}$) ($1\bar{1}3$) four-beam case for #A and #B samples. In other words, the multiple diffraction condition of this four-beam case is scanned in small steps. It provides a better visualization of the HR together with the exact four-beam case diffraction, as it can be seen in these figures. One can easily see the identified contributions of substrate (S), layer (L), hybrid (H) peaks and thickness interference fringing. From these two mappings, the effect of the layer thickness on the shape and intensity of the HR is clearly observed.

**Table 1** Results of the rocking curve characterization of #A and #B samples.

| samples | thickness (nm) | $x$ (Ga) | $a_\perp$ (Å) |
|---|---|---|---|
| #A | 58 | 0.458 | 5.6769(3) |
| #B | 360 | 0.434 | 5.6871(2) |

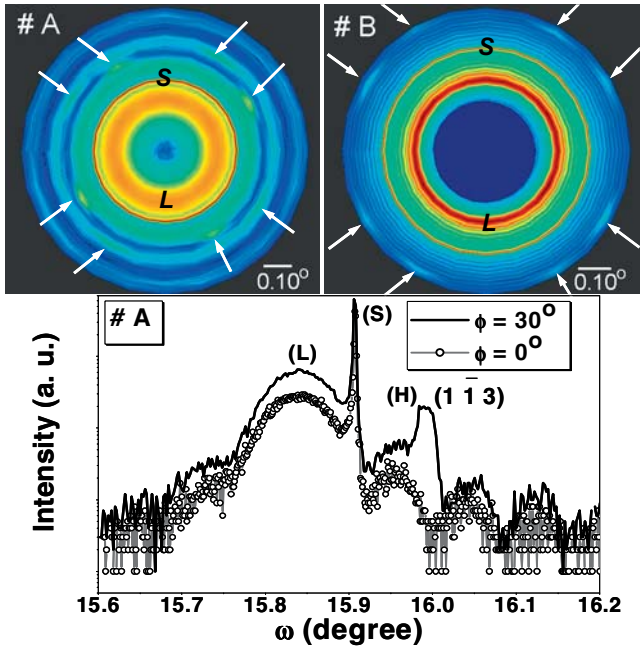


**Figure 3** (online colour at: www.pss-b.com) Synchrotron radiation pole diagrams of #A and #B samples with the substrate and layer contributions identified. Also shown is the rocking curve of #A for two azimuthal positions ($\phi$ = 0° and 30°) to enhance the SL hybrid contribution.

Sample #A presents a stronger HR broadening, along the substrate streak, due to its small layer thickness in comparison with sample #B. The observed distance between the substrate and the layer peak ($\Delta\omega$) is of the order of twice the distance between the substrate and the HR peak.

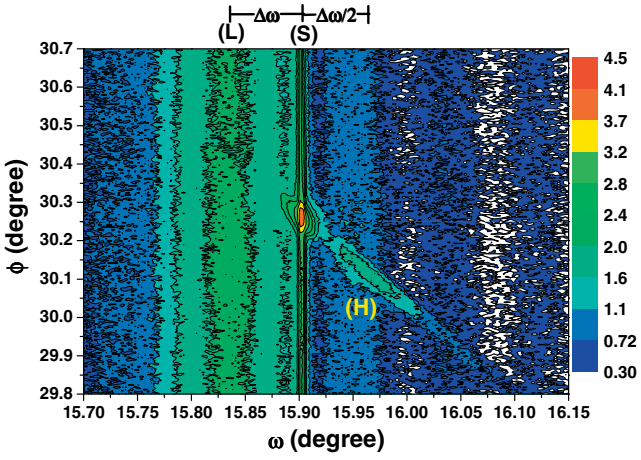


**Figure 4** (online colour at: www.pss-b.com) $\omega:\phi$ mapping of ($1\bar{1}\,\bar{1}$) ($1\bar{1}3$) four-beam case for #A sample with synchrotron radiation. Substrate, layer and hybrid contributions appear identified as well as their angular separation. One observes the elongation of HR contribution for the thinner layer.

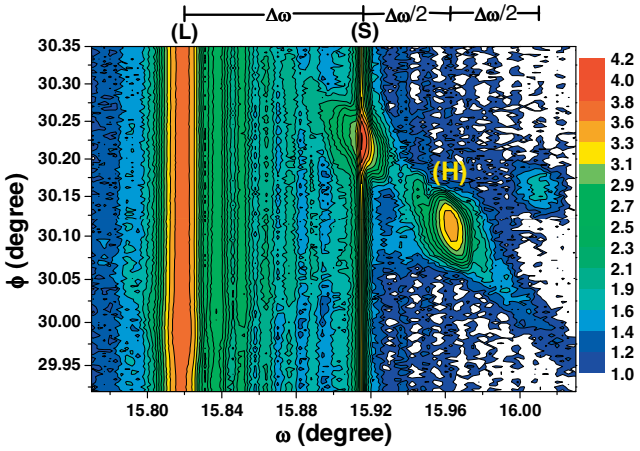


**Figure 5** (online colour at: www.pss-b.com) $\omega$:$\phi$ mapping of $(1\bar{1}\bar{1})$ $(1\bar{1}3)$ four-beam case for #B sample with synchrotron radiation. Substrate, layer and hybrid contributions appear identified as well as their angular separation. One observes the occurrence of a weaker additional HR to the right ($\Delta\omega/2$) of the SL hybrid contribution.

Moreover, in Fig. 5 (thicker layer) it is possible to observe another weaker HR at twice the angular separation of the stronger HR peak. It should be pointed out that HR peaks in Figs. 4 and 5 are of the SL type with pathway $H'_o = (1\bar{1}3)_S + (\bar{1}1\bar{1})_L$, confirmed by the ($\omega$, $\phi$) calculated positions which are (15.945°, 30.197°) for sample #A and, (15.964°, 30.116°) for sample #B. These values are in good agreement with the experimental $\omega$:$\phi$ mapping data.

**5 Conclusions** The direct observation of HRs in the InGaP/GaAs system provides an alternative and very useful tool to investigate three-dimensional structural properties of epitaxial layers, as thin as 58 nm, grown by CBE. The sample azimuthal homogeneity can be observed from the well defined rings in the pole diagram for both samples. The crystal truncation rod of the epilayer reciprocal lattice points introduces an elongation of the HR shape along the streak of the substrate secondary reflection, indicating in-plane match of the epilayer and substrate lattice parameters.

**Acknowledgments** The authors thank the Brazilian Agencies CNPq, CAPES, FAPESP and the support from the Laboratório Nacional de Luz Síncrotron (LNLS), Campinas, SP, Brazil.

## References

[1] L. H. Avanci, L. P. Cardoso, S. E. Girdwood, D. Pugh, J. N. Sherwood, and K. J. Roberts, Phys. Rev. Lett. **81**, 5426 (1998).
[2] L. H. Avanci, L. P. Cardoso, J. M. Sasaki, S. E. Girdwood, K. J. Roberts, D. Pugh, and J. N. Sherwood, Phys. Rev. B **61**, 6507 (2000).
[3] A. O. dos Santos, W. H. Yaegashi, R. Marcon, B. B. Li, R. V. Gelano, L. P. Cardoso, J. M. Sasaki, M. A. R. Miranda, and F. E. A. Melo, J. Phys.: Condens. Matter **13**, 10497 (2001).
[4] J. M. A. Almeida, M. A. R. Miranda, C. M. R. Remédios, F. E. A. Melo, P. T. C. Freire, J. M. Sasaki, L. P. Cardoso, A. O. dos Santos, and S. Kycia, J. Appl. Crystallogr. **36**, 1348 (2003).
[5] J. M. A. Almeida, M. A. R. Miranda, L. H. Avanci, A. S. de Menezes, L. P. Cardoso, and J. M. Sasaki, J. Synchrotron Radiat. **13**, 435 (2006).
[6] A. S. de Menezes, A. O. dos Santos, J. M. A. Almeida, J. M. Sasaki, and L. P. Cardoso, J. Phys.: Condens. Matter **19**, 106218 (2007).
[7] M. A. Hayashi, S. L. Morelhão, L. H. Avanci, L. P. Cardoso, J. M. Sasaki, L. C. Kretly, and S. L. Chang, Appl. Phys. Lett. **71**(18), 2614 (1997).
[8] R. V. Orloski, M. A. A. Pudenzi, M. A. Hayashi, J. W. Swart, and L. P. Cardoso, J. Mol. Catal. A, Chem. **228**, 177 (2005).
[9] S. L. Morelhão, L. P. Cardoso, J. M. Sasaki, and M. M. G. de Carvalho, J. Appl. Phys. **70**(5), 2589 (1991).
[10] S. L. Morelhão, L. H. Avanci, M. A. Hayashi, L. P. Cardoso, and S. P. Collins, Appl. Phys. Lett. **73**(15), 2194 (1998).
[11] M. Renninger, Z. Phys. **106**, 141 (1937).
[12] S. L. Morelhão and L. P. Cardoso, J. Appl. Phys. **73**, 4218 (1993); Solid State Commun. **88**, 465 (1993).
[13] S. L. Morelhão and J. Z. Domagala, J. Appl. Crystallogr. **40**, 456 (2007).
[14] S. Takagi, Acta Crystallogr. **15**, 1311 (1962).
[15] S. Takagi, J. Phys. Soc. Jpn. **26**, 1239 (1969).
[16] D. Taupin, Bull. Soc. Fr. Mineral. Cristallogr. **87**, 469 (1964).
[17] A. Pesek, P. Kastler, L. Palmetshofer, F. Hauzenberger, P. Juza, W. Faschinger, and K. Lischka, J. Phys. D, Appl. Phys. **26**, A177 (1993).

 